FABRICATION OF POROUS Al_2O_3-BASED CERAMICS USING COMBUSTION SYNTHESIZED POWDERS

#JIAHAI BAI, QINGYANG DU, GUOCHANG LI, CHENGFENG LI, YUNXIA ZHAO, JUNCHENG LIU

School of Materials Science and Engineering,
Shandong University of Technology, ZiBo, 255049,P. R. China

#E-mail: zbbjh@sdut.edu.cn

Submitted May 5, 2011; accepted November 28, 2011

Keywords: Combustion synthesis, Porous ceramics, Al_2O_3

Porous Al_2O_3-based ceramics were fabricated from powders synthesized via a solution combustion process using starch and urea as fuels. Effects of the relative fuel-to-oxidant ratio (φ_e = 1.4, 1.6, 1.8 and 2.0, respectively) on open porosity, pore size distribution and flexural strength of the as-prepared porous Al_2O_3-based ceramics were investigated. Experimental results revealed that the densification ability of the as-synthesized powders increased significantly as φ_e increased, and open porosity, pore size distribution and flexural strength of the porous ceramics exhibited remarkable dependence on the densification ability of the powders instead of the weight fraction of the charred organic residuals in the powders. SEM micrographs disclosed that the porous ceramics from the precursors with φ_e = 1.8 or 2.0 exhibited significantly homogenous microstructures including pore size and pore distribution.

INTRODUCTION

Porous ceramics have attracted increasing attention due to their wide applications in many industrial areas, such as catalyst carriers, membrane supports, filters and biomaterials [1-4]. These applications usually require that porous ceramics have many excellent properties concerning microstructures, porosity and mechanical strength, etc. [5]. Thus, many routes, e.g., freeze casting [6-8], gelcasting [9, 10], ice templating [11, 12] and starch consolidation casting [13, 14] were explored to regulate the properties of porous Al_2O_3 ceramics. At the same time, some novel precursors for Al_2O_3 powders and nanometer alumina were employed to fabricate porous Al_2O_3 ceramics. For example, dried boehmite gel [15], $Al(OH)_3$ [16,17], Al_2O_3 sol [18] and nanometer alumina [19] were used to prepare porous Al_2O_3 ceramics. It has been shown that the starting materials play a crucial role in enhancing the properties of porous Al_2O_3-based ceramics. Thus, preparation of appropriate precursors is essential to tailor properties of porous Al_2O_3-based ceramics.

Solution combustion synthesis, a novel wet chemical method, has many advantages including high sinterability, convenient processing, simple experimental setup, significant time-saving and potential large-scale production, etc [20, 21]. So many investigations were carried out to synthesize Al_2O_3 powders using the solution combustion technique in recent years [22-25]. However, fabrication of porous Al_2O_3 Al_2O_3-based ceramics from the combustion synthesized powders was not reported in the above-mentioned papers.

In the present work, porous Al_2O_3-based ceramics with homogenous microstructures concerning pore size and pore distribution were fabricated from solution combustion synthesized powders. Furthermore, effects of the relative fuel-to-oxidant ratio of the precursors on properties of the as-fabricated porous ceramics were investigated.

EXPERIMENTAL

Combustion synthesis

Reagents used in the present work are analytically pure and no further purification was made. Powders for the porous ceramics were synthesized via a solution combustion route using $Al(NO_3)_3{\cdot}9H_2O$, $Mg(NO_3)_2{\cdot}6H_2O$ as oxidants, and urea ($CO(NH_2)_2$) and soluble starch ($(C_6H_{10}O_5)_n$) as fuels. It is worth noting that the precursors were designed to containing additional 5 mol% $Mg(NO_3)_2{\cdot}6H_2O$ to achieve homogenous microstructures concerning pore size and Al_2O_3 grain size.

A typical experimental procedure was as follows: First, 0.10 mole $Al(NO_3)_3{\cdot}9H_2O$, 0.005 $Mg(NO_3)_2{\cdot}6H_2O$ and 0.25 mol urea were dissolved into 50 ml deionized water, followed by adding soluble starch (4.06, 6.09, 8.12 and 10.15 g, respectively) into the solutions preheated to 70°C. Subsequently, the solutions were vaporized at 60°C under magnetic stirring until gels were formed. Then the aqueous mixtures were heated in a domestic microwave oven using its maximum power (800 W). Under microwave irradiation, the aqueous precursor boiled, swelled, evolved a large amount of gases and

finally ignited, yielding foam-like powders. Finally, the powders were dry-milled for 1 h in a planetary ball mill using zirconia ball as milling media at a rotation speed of 200 rpm.

To explain the redox properties of the aqueous precursors, the relative fuel-to-oxidant ratio (φ_e) [26] was used and calculated using the following equation:

$$\varphi_e = \frac{m\times\{6\cdot 4_C+10\cdot 1_H+5\cdot(-2)_O\}+0.25\cdot\{(1\times 4_C+1\cdot(-2)_O+2(1\cdot 0_N+2\cdot 1_H)\}}{(-1)\{0.10\cdot\{1\cdot 3_{Al}+3(1\cdot 0_N+3\cdot(-2)_N)\}+0.005\cdot\{1\cdot 2_{Mg}+2(1\cdot 0_N+3\cdot(-2)_O)\}\}} \quad (1)$$

where m is the mole number of $C_6H_{10}O_5$, i.e., the monomer of starch in four precursors, 0.25, 0.10 and 0.005 are the mole number of $CO(NH_2)_2$, $Al(NO_3)_3\cdot 9H_2O$ and $Mg(NO_3)_2\cdot 6H_2O$ in the precursors, respectively. Noted that φ_e is determined by dividing the sum of total valences of oxidizing elements and reducing elements in the fuels (e.g., urea and starch) by that in the oxidants (e.g., $Al(NO_3)_3\cdot 9H_2O$ and $Mg(NO_3)_2\cdot 6H_2O$). In this type of calculation, oxygen is the only oxidizing element and has a negative valence, carbon, hydrogen, and metal caions are reducing elements and have positive valences, and nitrogen is considered as neutral and has a zero valence [26]. For the purpose of convenient and lucidity, The valences of O, N, H, C, Al and Mg elements in fuels and/or oxidants are expressed as $(-2)_O$, 0_N, 1_H, 4_C, 3_{Al} and 2_{Mg}, respectively, as shown in Equation 1.

A redox mixture is considered to be stoichiometric when $\varphi_e = 1$, fuel lean when $\varphi_e > 1$ and fuel rich when $\varphi_e < 1$. Theoretically, a stoichiometric redox mixture could produce maximum energy during combustion and thus lead to the highest flame temperature. Furthermore, if $\varphi_e > 1$ or $\varphi_e < 1$, as φ_e increases or decreases, combustion reactions would become more incomplete, thus flame temperature would become lower and more charred organic materials would be produced [26].

In this work, φ_e of four precursors is designed as 1.4, 1.6, 1.8 and 2.0, respectively. Hereinafter, the four as-fabricated powders/ceramics are termed powder/ceramics A, B, C and D, respectively.

Fabrication and characterization of porous ceramics

The as-prepared powders were granulated in a agate mortar using PVA (8 wt%) as binder and subsequently sieved through a 40-mesh screen. Then the powders were bidirectionally pressed into rectangular specimens with the size of 70.0 mm × 10.0 mm× 10.0 mm under the pressure of 50 MPa. After drying at 50°C for 12 h, the compacts were heated up to 1000°C at a heating rate of 1.0°C min^{-1} and then to 1400°C at a heating rate of 2.0°C min^{-1} in air, followed by soaking for 2 h at the peak temperature.

Ignition losses of the combustion-synthesized powders were determined by annealing them at 1000°C for 2 h. Water absorption, open porosity, bulk density of the porous ceramics were determined by the Archimedes method using distilled water as liquid medium. Linear firing shrinkage was simply calculated by measuring the length of the specimens before and after sintering. Flexural strength was tested via a three-point bending test (ATOGRAPH AG-I, Shimadzu) with a support distance of 30.0 mm and a cross-head speed of 0.50 mm/min. The crystalline phases were identified using an X-ray diffractometer (XRD, D8 Advance, Brucker, Germany), equipped with a Ni-filtered Cu Kα radiation source (λ = 0.154178 nm). The microstructures of the porous ceramics were characterized with a field emission scanning electron microscope (FESEM, Sirion 2000, FEI, Netherlands). Pore size distribution was determined with mercury porosimetry (Poremaster-60, Quantachrome, USA).

RESULTS AND DISCUSSION

XRD analysis

Figure 1 shows the XRD patterns of crystalline phases of the sintered ceramics from the combustion synthesized powders A and D. As shown in Figure 1, the characteristic peaks of the a-Al_2O_3 (corundum, JCPDS 46-1212) were indexed in the two patterns. In addition, a small amount of $MgAl_2O_4$ (JCPDS 21-1152) were also identified, as a result of addition of 5 mol% $Mg(NO_3)_2\cdot 6H_2O$ to the precursors. Therefore, it was concluded that Al_2O_3 ceramics with spinel phase were successfully fabricated from the combustion synthesized powders.

Properties of porous ceramics

The ignition losses (IL) of combustion-produced powders and properties of the as-prepared ceramics are summarized in Table 1. As can be seen from Table 1,

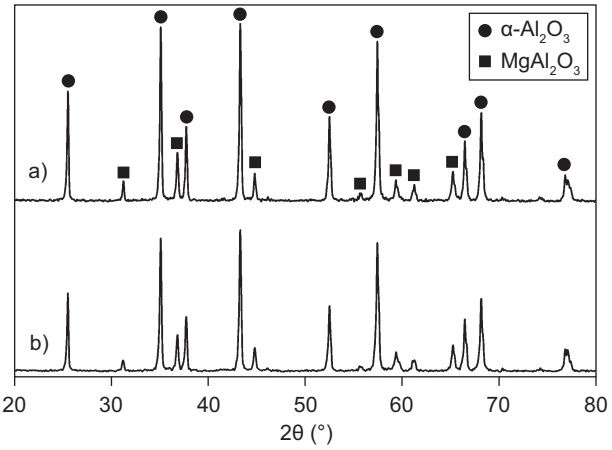

Figure 1. XRD patterns of crystalline phases of porous Al_2O_3-based ceramics A: (a) and D: (b) from precursors with φ_e equal to 1.4 and 2.0, respectively.

the combustion synthesized powders all exhibited considerable ignition losses. Moreover, the ignition losses of the powders increased from 11.3 wt.% to 49.6 wt.% as φ_e of the precursors rose from 1.4 to 2.0, indicating that a large amount of (partly) charred organic materials were produced during combustion owing to the incomplete redox reactions of metal nitrate to fuels. Meanwhile, when φ_e rose from 1.4 to 2.0, water absorption (W.A.) and open porosity (O.P.) of the as-prepared ceramics decreased from 34.6 % and 60.1 % to 12.0 % and 31.0%, respectively, while bulk density (B.D.) and the relative density (R.D.) of the Al_2O_3-based ceramics increased from 1.7 g cm^{-3} and 43.5 % to 2.6 g cm^{-3} and 64.3 %, respectively. Moreover, the linear firing shrinkage (L.F.S) of the porous ceramics increased from 12.2 % to 33.2 % as φ_e ascended from 1.4 to 2.0, implying that the densification ability of the as-synthesized powders was remarkably increased as φ_e rose. The flexural strength (F.S.) of the porous ceramics increased from 2.1 MPa to 7.3 MPa when φ_e arose from 1.4 to 1.8, which was mainly ascribed to the increasing degree of densification.

Generally, voids are formed in porous ceramics as organic materials are burned out at high temperatures. Thus, it was expected that more charred organic residuals in the as-synthesized powders would lead to larger open porosity of the as-prepared porous Al_2O_3-based ceramics. However, the degree of densification of the porous ceramics was remarkably increased and their open porosity was markedly decreased, though the ignition losses of the combustion-synthesized powders increased sharply as φ_e rose. Therefore, open porosity of the porous ceramics was mainly dependent on the densification ability of the combustion-synthesized powders instead of the weight/volume fraction of the charred organic residuals in the powders. Moreover, according to the trend in evolution of open porosity and the linear firing shrinkage of the porous ceramics listed in Table 1, it could be inferred that the densification ability of the combustion produced powders is sharply increased with φ_e rising. Since the redox precursors become fuel leaner when φ_e increases from 1.4 to 2.0, combustion reactions would become more incomplete. As a result, the flame combustion temperature would be lowered and more charred organic materials were produced in the as-prepared powders [26]. Therefore, the reactivity of the as-synthesized powders became higher as φ_e increased. Hence, open porosity and water absorption of the porous ceramics decreased as φ_e increased.

Pore size distribution

Figure 2 depicts the pore size distribution of the porous Al_2O_3-based ceramics from the combustion synthesized powders. As shown in Figure 2, the peak of the pore size distribution moved forwards from 5.5 μm to 0.25 μm as φ_e of the precursors increased from 1.4 to 2.0. In addition, the pore size distribution of the porous Al_2O_3-based ceramics become much narrower with φ_e rising. This trend in evolution of the pore size distribution was, at least partly, attributed to the fact that the degree of densification of the porous Al_2O_3-based ceramics increased as φ_e rose from 1.4 to 2.0.

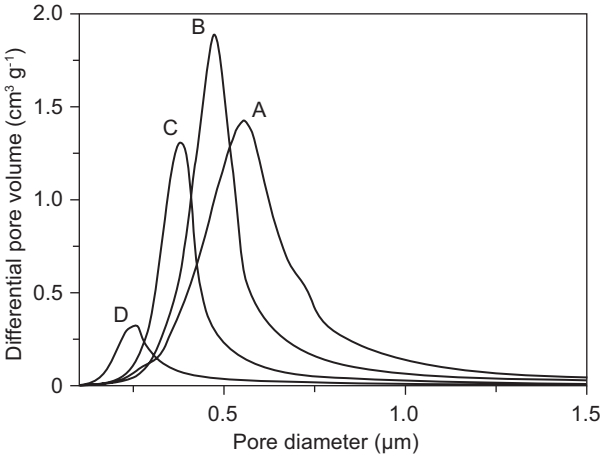

Figure 2. Pore size distribution of porous Al_2O_3-based ceramics A, B, C and D from precursors with φe equal to 1.4, 1.6, 1.8 and 2.0, respectively.

SEM microstructures

Figure 3 shows the SEM micrographs of the fracture surfaces of the porous ceramics A, C and D. As shown in Figure 3, a large number of pores were all observed on the fracture surfaces of the three porous Al_2O_3-based ceramics. However, there were still remarkable differences in the microstructures of the porous Al_2O_3-based ceramics. For the porous ceramics A, there were a larger amount of submicron-sized pores on its fracture surfaces as well as a little larger pores with their diameters in the range of 1.5~5 μm. However, the volume fraction of these larger pores was far less, as shown in Figure 3a, so they were not presented in the pore size distribution

Table 1. Properties of the combustion synthesized powders and the porous Al_2O_3-based ceramics

Ceramics	φ_e	IL (wt%)	L.F.S. (%)	W.A. (%)	O.P. (%)	B.D. (g cm^{-3})	F.S. (MPa)
A	1.4	11.3	12.2	34.6±1.4	60.1 ±3.5	1.7±0.1	2.1 ±0.3
B	1.6	19.9	15.2	32.0±1.0	57.1±2.1	1.8±0.1	3.5 ±0.5
C	1.8	38.3	24.3	23.9±2.2	48.2±3.8	2.0±0.1	7.3±0.7
D	2.0	49.6	33.2	12.0±1.1	31.0±1.6	2.6±0.1	–

shown in Figure 2. At the same time, the average pore size of the ceramics C and D were much smaller than that of ceramics A. Moreover, pore size and pore distribution of the former was much more homogeneous as compared with the latter. The average pore size and porosity of the ceramics C were remarkably smaller than those of the ceramics D, agreing well with the pore size distribution shown in Figure 2, though the microstructures of the ceramics C and D were somewhat similar. As shown in Figure 3a,b (there were considerable porous grain agglomerates on the fracture surfaces of the ceramics A. The grain agglomerates appeared to be relatively

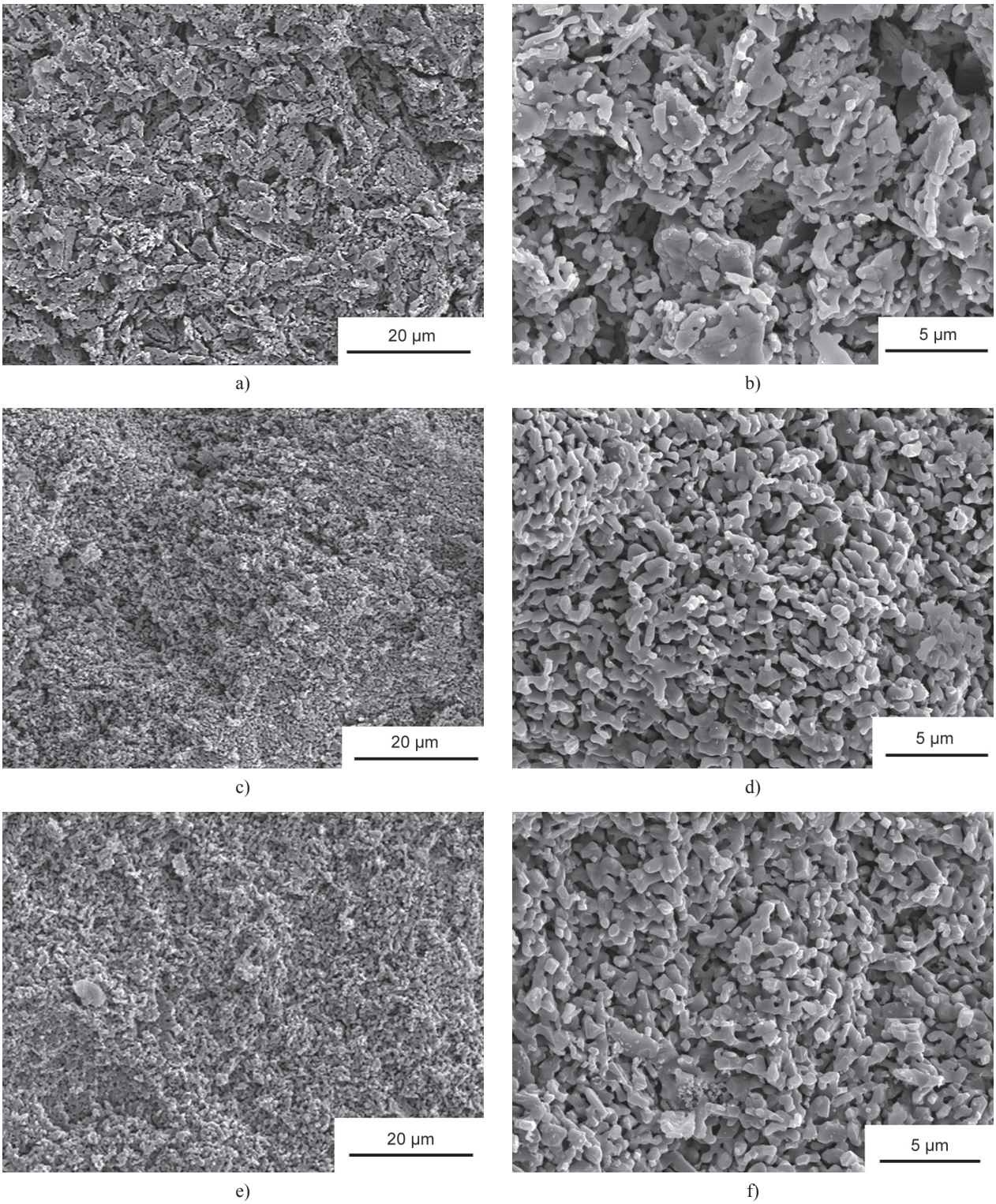

Figure 3. SEM micrographs of the fracture surface of porous Al_2O_3-based ceramics. (a, b), (c, d) and (e, f), porous ceramics A, C and D from precursors with φ_e equal to 1.4, 1.8 and 2.0, respectively.

isolated by pores, and the connections between these agglomerates were much weaker. On the contrary, as presented in Figure 3c-f, most grains were integrated into a net-like structure and no appreciable grain agglomerates were observed in the porous ceramics C and D. Nevertheless, the contacts of grains within agglomerates in the ceramics A exhibited no appreciable difference from those in the ceramics C and D. Thus, weaker connections between the agglomerates as well as higher porosity and larger average pore size were mainly responsible for the lower flexural strength of the porous ceramics A, as compared with the ceramics C.

CONCLUSIONS

Porous Al_2O_3 ceramics containing spinel phase were successfully fabricated from the powders synthesized via a combustion route using urea and starch as fuels. The densification ability of the as-synthesized powders increased significantly as the relative fuel-to-oxidant ratio of the precursors rose from 1.4 to 2.0. Open porosity and the average pore size decreased, bulk density and flexural strength of the porous Al_2O_3-based ceramics increased, though the ignite losses of the as-synthesized powders became larger as φ_e rose. Open porosity, pore size distribution and the flexural strength of the porous ceramics exhibited remarkable dependence on the densification ability of the combustion-synthesized powders instead of the weight fraction of the charred organic materials in the powders. In addition, the porous ceramics C and D exhibited significantly homogeneous microstructures including pore distribution and pore size.

Acknowledgement

The author gratefully acknowledges the financial support by the Natural Science Foundation of Shandong Province, China (Grant No: ZR2010EL007).

References

1. Ismagilov Z.R., Shkrabina R.A., Koryabkina N.A., Kirchanov A.A., Veringa H., Pex P.: React. Kinet. Cata. Lett. *60***,** 225 (1997).
2 Jo Y.M., Hutchison R.B., Raper J.A.: Powder Technol. *91*, 55 (1997).
3. Then P.M., Day P.: Interceram. *49*, 20 (2000).
4. Yoon B.H., Choi W.Y., Kim H.E., Kim J.H., Koh Y.H.: Scripta Mater. *537*, 58 **(**2008**)**.
5. Ishizaki K., Komarneni S. and Nanko M.: *Porous Materials, Process Technology and Applications,* p. 181-198, Kluwer Academic Publishers, London 1998.
6. ZhangY.M., Hu L.Y., Han J.C., Jiang Z.H.: Ceram. Int. *36*, 617 (2010).
7. Jing L., Zuo K.H., Zhang F.Q., Chun X., Fu Y.F., Jiang D.L., Zeng Y.P.: Ceram. Int. *36*, 2499 (2010).
8. Lu K., Kessler C.S., Davis R.M.: J. Am. Ceram. Soc. *89*, 2459 **(**2006)
9. Takahashi M., Menchavez R.L., Fuji M., Takegami H.: J. Eur. Ceram. Soc. *29*, 823 (2009).
10. Ortega F.S., Sepulveda P., Pandolfelli V.C.: J. Am. Ceram. Soc. *22*, 1395 (2002).
11. Zhang D., Meggs C., Button T.W.P.: Scripta Mater. *62*, 466 (2010).
12. Nishihara H., Mukai S.R., Fujii Y., Tago T., Masuda T., Tamon H.: J. Mater. Chem. *31*, 3231 (2006).
13. Bhattacharjee S., Besra L., Singh B.P.: J. Eur. Ceram. Soc. *27*, 47 (2007).
14. Gregorova E., Pabst W.: J. Eur. Ceram. Soc. *27*, 669 (2007).
15. Kawamura K. and Endo H.: J. Ceram. Soc. Jpn. *104***,** 734 (1996).
16. Deng Z.Y., Fukasawa T., Ando M., Zhang G.J., Ohji T.: J. Am. Ceram. Soc. *84*, 485 (2001).
17. Deng Z.Y, Fukasawa T., Ando M., Zhang G.J., Ohji T.: J. Am. Ceram. Soc. *84*, 26.
18. Kritikaki A., Tsetsekou A.: J. Eur. Ceram. Soc. *29*, 1603 (2009).
19. Li G.H., Jiang Z., Jiang A.Q. and Zhang L.D.: Nanostruct. Mater. 8, 749 (1997).
20. Aruna S.T., Mukasyan A.S.: Curr. Opin. Solid. ST. M. *12*, 44 (2008).
21. Patil K.C., Aruna S.T., Mimani T.: Curr. Opin. Solid. ST. M. *6*, 507 (2002).
22. Chen C.C., Huang K.T.: J. Mater. Res. *424*, 20 **(**2005**).**
23. Toniolo J.C., Lima M.D., Takimi A.S., Bergmann C.P.: Mater. Res. Bull. *40*, 561 (2005).
24. Peng T.Y., Liu X., Dai K., Xiao J.R., Song H.B.: Mater. Res. Bul. *41*, 1638 (2006).
25. Ganesh I., Torres P.M.C., Ferreira J.M.F.: Ceram. Int. *35*, 1173 (2009).
26. Patil K.C., Hegde M.S., Rattan Tanu, Aruna S.T.: *Chemistry of Nanocrystalline Oxide Materials: Combustion Synthesis, Properties and Applications*, p. 42-45, World Scientific, Singapore 2008.